Magnetic Bistability of Co Nanodots

H. F. Ding,[1] A. K. Schmid,[2] Dongqi Li,[1] K. Yu. Guslienko,[1] and S. D. Bader[1]

[1]*Materials Science Division, Argonne National Laboratory, 9700 South Cass Avenue, Argonne, Illinois 60439, USA*
[2]*Materials Sciences Division, Lawrence Berkeley National Laboratory, 1 Cyclotron Road, Berkeley, California 94720, USA*

(Received 28 May 2004; revised manuscript received 30 November 2004; published 20 April 2005)

Size-dependent magnetic single-domain versus vortex state stability of Co/Ru(0001) nanodots is explored with spin-polarized low-energy electron microscopy, analytical modeling, and micromagnetic simulations. We show that both single-domain and vortex states can be stabilized in a broad region near the phase boundary. The calculated width of the bistability region and temperature dependent heights of the energy barriers between both states agree well with our experimental findings.

DOI: 10.1103/PhysRevLett.94.157202 PACS numbers: 75.30.Kz, 42.65.Pc, 61.46.+w, 75.70.Kw

Recently, magnetic structures with dimensions on the nanometer scale have drawn increasing attention due to the opportunity to exploit their applications and understand their physical phenomena. The magnetic properties of small elements are usually governed by their shape, size, and material parameters. Below a critical dimension, they are usually in magnetic single-domain (SD) states [1,2]. Above that, magnetic domains occur in order to reduce the magnetostatic energy. Competition between the exchange energy and the magnetostatic energy governs the transitions between SD and multidomain states. One particular class of transitions, between SD and vortex (V) states, has recently been discussed extensively. Analytical models and micromagnetic simulations have been developed to predict phase diagrams for magnetic nanostructures as a function of their dimensions [3–9]. It was found that the existence of in-plane anisotropy strongly favors SD states [6], while perpendicular anisotropy has little influence on the phase diagrams [7]. With increasing control of fabrication processes and advances of magnetic imaging techniques, it has become possible to explore the phase diagrams experimentally [8–12]. However, the lack of agreement between the experiments and theoretical predictions still poses challenges [8–10].

In this Letter, we carry out a joint experimental and theoretical study using Co nanodots epitaxially grown on Ru(0001). We used spin-polarized, low-energy electron microscopy (SPLEEM) to monitor the growth and magnetic structure of dots during *in situ* preparation. By controlling substrate temperature and Co dose, different sizes of dots (20–800 nm wide, 1–4 nm thick) are created and investigated. The SPLEEM images show that the as-grown Co dots are generally in SD states with the magnetization oriented randomly in the film plane. Analytical modeling and micromagnetic simulations, however, suggest that V states are the ground states for larger dots. To explain the discrepancy, a newly extended phase diagram with magnetic bistability near the phase boundary is proposed. A key feature of the diagram is that stability regions of the V and SD states overlap substantially and there are size-dependent energy barriers between the states. Consistent with this new picture, we find that the Co dots can be converted from a SD state into a V state with thermal annealing. Our calculations and experiments demonstrate the general concept of bistability and the possibility to overcome energy barriers between magnetic states by thermal activation.

Co dots have been grown with molecular beam epitaxy on Ru(0001) in ultrahigh vacuum at temperatures from 600 to 860 K. Details on sample growth can be found in Ref. [13]. For each temperature, we continuously monitor both the growth and the magnetic structure of the dots as a function of the Co dosage with SPLEEM, using an acquisition rate of 1 frame/s [where ≈ 60 frames correspond to 1 monolayer (ML)]. We outline features of the SPLEEM techniques that are useful in our study below [14]. A beam of spin-polarized, low-energy electrons is backscattered at the sample surface and is collected to form images. Surface morphology, chemical composition, and sample magnetization give rise to the contrast in these images, which is useful to monitor the shapes and dimensions of Co nanodots. The spin direction of the beam is varied and one records pairs of images using oppositely polarized beams. When pixel-by-pixel difference images are computed from such pairs, contrast due to surface morphology and composition is canceled, and only magnetic contrast MC is visible. The MC is proportional to the dot product of the local magnetization vector $\vec{M}$ and the spin-polarization vector $\vec{S}$ of the illuminating electron beam, $MC \propto \vec{M} \cdot \vec{S}$, which allows one to determine the orientation of the local magnetization in the sample surface.

We find that Co deposition at a temperature below 650 K results in continuous films. Above 700 K, Co first forms a 1-ML thick wetting layer. Islanding then starts with continued deposition, resulting in the formation of nanodots. The lateral sizes of the Co dots increase with the Co dose, typically in the range of 20–800 nm. For a given dosage, the dots are larger for higher temperatures. An image acquired after nominally 3 ML of Co were deposited at 780 K [see Fig. 1(a)] shows the typical morphology of the

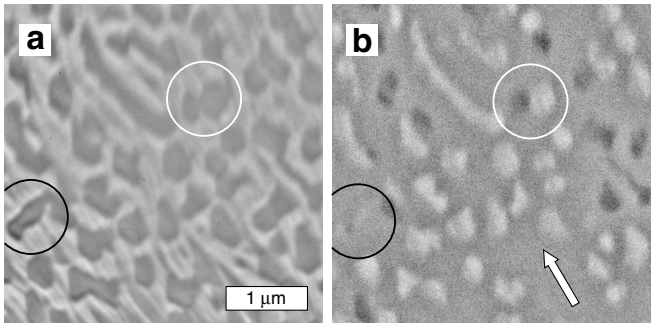

FIG. 1. Morphology (a) and magnetic image (b) of Co dots deposited at 780 ± 10 K on a Ru(0001) substrate obtained by SPLEEM. The Co equivalent thickness is ≈ 3 ML. The arrow in (b) indicates the magnetization orientation of the bright domains. For the meaning of the inserted circles, see text.

Co dots with many dark dots decorating a gray background. The background is the Ru covered by a 1-ML Co wetting layer. The dark dots are Co islands with an average size of 400 ± 100 nm. A typical size and height distribution of the dots was presented in Ref. [15]. From a measurement of the area fraction covered with islands and the total Co dosage, we estimate that the average island height in this example is ≈ 1 nm. Most of the islands are isolated and have sixfold symmetric shape. Figure 1(b) shows a magnetic image of the same area. The white arrow near the bottom of the image indicates the magnetization orientation of the bright gray domains. With few exceptions, each Co island appears in a homogeneous shade of gray; i.e., the dots are in magnetic SD states. A few dots have merged with neighbors, such as the feature marked by white circles; only in these rare cases one can observe multidomain configurations. Recalling that the magnetic contrast is $\propto \vec{M} \cdot \vec{S}$, one can understand the different shades of contrast in Fig. 1(b). Individual islands appear in different shades of gray, and a comparison of the SPLEEM image (b) with the morphology image (a) reveals extreme examples, such as an island marked by a black circle in (a). It appears to be missing in (b), which indicates that its magnetization is oriented perpendicular to the spin axis of the electron beam. The observations suggest that the individual dots are in SD states with magnetization oriented randomly in the film plane indicating weak in-plane magnetic anisotropy. By controlling Co dose and substrate temperature (700–860 K), dots with different dimensions (20–800 nm wide and 1–4 nm thick) are created and investigated. Most of the as-grown dots are found in SD states and none are in V state.

It was proposed that, depending on geometric and material parameters, a magnetic instability of SD versus V states can exist and that domain states can be switched by applying an external magnetic field [10,13]. In the present study, we focus on a thermally activated magnetic transition. We observe that dots found in SD states can be switched to V states by annealing, and V states can be switched to SD by applying in-plane magnetic field pulses. We have documented multiple transitions of many individual dots. For example, the sample shown in Fig. 1 was annealed to 940 K in ~50 K steps, and then cooled to the temperature used for imaging the as-grown Co dots. Below 940 K, no thermal activated switching was found. To exclude other unwanted effects, such as Co desorption and change of the dot dimension and shape, we avoided overheating. Figure 2 shows a magnified view of Co dots after annealing. The morphology image shown in Fig. 2(a) indicates that there is no significant change of dot shape and size. (Enhanced dark contrast on upper and lower edges are an artifact due to imperfect stigmatism of optics.) The SPLEEM images (b)–(d) show bright and dark contrast, separated by gray contrast. The magnetization at certain edges is perpendicular to the incoming electron spin axes, and therefore the edges are invisible, which makes the magnetic image appear to slightly deviate from the topological symmetry. Taken alone, one such image consisting of bright and dark contrast could be interpreted as showing either two domains separated by a domain wall, or a V structure. We took several images with different spin axes of the electron beam to eliminate this ambiguity and prove the existence of V states. For the two-domain case, the strength of the contrast might change, but the orientation of the domains would remain unchanged. SPLEEM images of a V state appear rotated when the spin axis of the beam is rotated, while the strength of the contrast remain unchanged. Figures 2(b)–2(d) present the images obtained with the electron beams in different spin axes (marked by white arrows). The rotation of contrast along with the spin axis proves that the dot is, indeed, in a V state. In this way, we have tracked the magnetic domain state histories of specific dots through alternating thermal

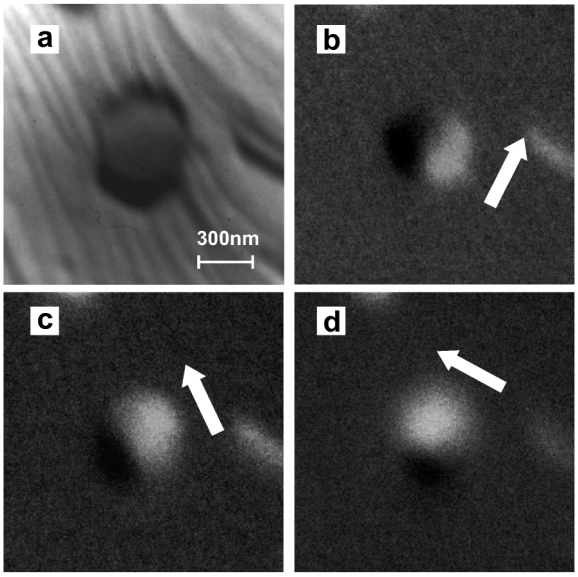

FIG. 2. Morphology (a) and magnetic images (b)–(d) of the same sample shown in Fig. 1, after annealing at 940 ± 10 K. The arrows in (b)–(d) indicate the magnetization orientation of the bright region in each panel.

and magnetic field cycles. In one typical experiment, we identified 90 dots in a V state after annealing. After an in-plane field pulse with strength of ~1300 Oe and width of 1–2 s, 50 of these dots switched to SD states. After an additional annealing cycle, 25 of these particular SD dots transformed back to V states. The measured histories of a statistically significant number of dots clearly suggest bistability of the system.

To understand the magnetic behavior of the system, we carried out both analytical calculations and micromagnetic simulations utilizing the OOMMF code [16]. In the simulations, we model the dots as hexagonal prisms, which is similar to the shapes found experimentally. We ignore interactions between dots, as we discussed previously [13] that interactions are only significant in populations of more closely spaced dots. We also assume the 1-ML wetting layer is nonmagnetic as we do not observe any magnetic signal on it. The parameters used for the calculations are taken from Brillouin light scattering measurements for hcp Co [17], where $A = 2.5 \times 10^{-11}$ J/m for the exchange constant, $M_s = 1.4 \times 10^6$ A/m for the saturation magnetization, and $K_1 = 5.3 \times 10^5$ J/m^3 for the uniaxial anisotropy along the c axis. First, simulations are carried out to estimate the equilibrium boundary between the SD and V states. For this, we compare the total energy for both SD and V states and find the critical dimensions where the total energies for both states are equal. In these calculations, the cell size is selected to be $2 \times 2 \times 1$ nm^3, which is much smaller than the exchange length $L_{\mathrm{ex}} = \sqrt{8\pi A/\mu_0 M_s^2}$ (≈ 16 nm for Co) with μ_0 being the permeability of vacuum. The results are summarized in Fig. 3 as open circles. On first thought, the result may seem surprising as our experimental data show that usually the as-grown Co dots are in SD states, even in the case of some dots with lateral sizes as large as 800 nm and height of 4 nm. The simulations, however, also suggest bistability of the system; i.e., both SD and V states can be stable near the energy equilibrium boundary. To explore the bistability of the system, we also calculate two other boundaries, i.e., the lower boundary where V states turn into SD states (solid squares in Fig. 3), as well as the upper boundary where SD states split into V or other multidomain structures (solid triangles in Fig. 3). This is done by initializing the state to be a V for lower boundary and SD for upper boundary and by observing the final state until they are unstable. In addition, open triangles represent transitions from the in-plane SD to perpendicular SD phase. Our simulations indicate that both SD and V states are indeed expected to be stable in a broad region. The lateral size region in which both states can be stable extends from 45 to ~700 nm for 8 nm thick dots and 38 to ~1600 nm for 4 nm thick dots. This explains our experimental findings. In the early phase of the growth, Co dots are small and they start out naturally in SD states, as this is the only stable state. With increasing size, the dots tend to remain in their original states (SD) throughout the bistability region, until the energy minimum corresponding to SD state disappears. This picture explains the experimental observation that the as-grown dots tend to be in SD states despite the theoretical prediction that V states are the ground states for larger dimensions.

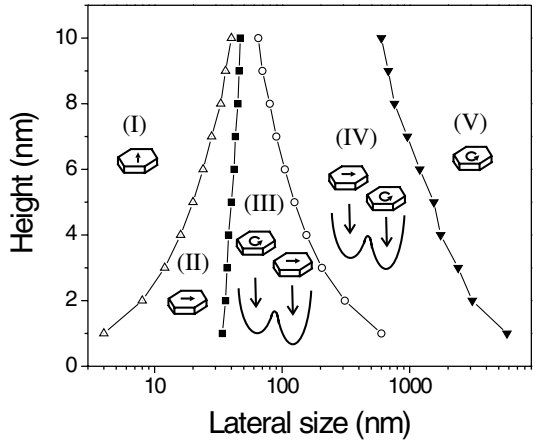

FIG. 3. Thickness and lateral size-dependent magnetic multiphase diagram of thin hexagonal Co dots obtained from micromagnetic simulations. In regions (I) and (II), perpendicular and in-plane single domains are the only stable states, respectively. Both in-plane single-domain and vortex states are stable in regions (III) and (IV) with the single domain and vortex being the ground state in (III) and (IV), respectively. In region (V), single-domain states are unstable, and vortex and other multidomain configurations are favored.

In the region of bistability, the SD and V states correspond to two distinct energy minima separated by a barrier. The height of the energy barrier is difficult to compute using micromagnetic simulations; therefore we take an analytical approach. To calculate the energy barriers, one needs to search for a path from one energy minimum to another one via a saddle point in multidimensional space. For the case of an uniaxial SD magnetic particle, this has been solved analytically for the field parallel to the anisotropy axis [18,19] and numerically for the nonaxial field [20]. The solution of the corresponding Fokker-Planck equation for the probability of different orientations of the particle magnetic moment leads to the well-known exponential dependence of the relaxation time on the energy barrier height. We explore here the thermally activated transition which involves a strongly nonuniform (V) state, whereas only coherent magnetization rotation was considered previously. For simplicity, we do not include the detailed hexagonal shape of the Co dots. Instead, a circular cylinder with radius R and height L is considered. Also, the influence of the anisotropy on the stability of the V and the in-plane SD states is neglected due to the small size of the V core in comparison with the dot radius. In the calculation, the position of the V center (l) with respect to the center of the cylindrical particle is used as the main parameter of the magnetization distribution. This permits a convenient description for both the V and the quasiuniform SD state as particular cases. We assume that the dot radius

is much larger than the V core radius, which is of the order of the exchange length. In this case, we can neglect changes of vortex shapes upon shifting the V from the dot center. Vortex states (shifted or centered) correspond to parameter $l < R$. The in-plane SD state corresponds to $l \gg R$, or the center of a fictitious V is located outside the dot, far from the particle border. We assume that the metastable SD state evolution path to the stable V state under thermal fluctuations corresponds to the movement of the V center from infinity to the center of the dot. We also assume that dot volume is not very large and that the reversal from the SD state to the V state can be described as a nonuniform, nonlocalized mode, and the energy barrier is then proportional to the particle volume Ω. We calculate the total magnetic energy density (in units of $M_s^2\Omega$) of the shifted V in the form,

$$W(s) = W(0) + \frac{1}{2r^2}\ln(1 - s^2) + 2\pi F(\beta)s^2\left(1 - \frac{1}{4}s^2\right),$$

where $s = l/R < 1$, $r = R/L_{\mathrm{ex}}$, $\beta = L/R$, and $F(\beta) = \int_0^\infty dt t^{-1} f(\beta t) J_1^2(t)$ [21]. Inside, $f(x) = 1 - [1 - \exp(-x)]/x$ and $J_1(x)$ is the first order Bessel function. With this, we can obtain the position of the energy maximum $s_m(\beta, r)$ as a function of the dot sizes:

$$s_m(\beta, r) = \frac{3}{2} - \frac{1}{2}\left(1 + \frac{2}{\pi F(\beta) r^2}\right)^{1/2}.$$

The typically value of s_m is 0.8–0.9. The energy of the in-plane SD state is $W_{\mathrm{SD}} = 2\pi F(\beta)$. The energy barriers for transitions SD $\rightarrow$ V and V $\rightarrow$ SD are different; they are $\Delta E_{sv}/M_s^2\Omega = W(s_m) - W_{\mathrm{SD}}$ and $\Delta E_{vs}/M_s^2\Omega = W(s_m) - W(0)$, respectively, which we will see makes it difficult to thermally cycle between states.

The calculated energy barriers for SD-V transitions show that the relaxation time $\tau = \tau_0 e^{\Delta E/k_B T}$ decreases rapidly with increasing dot size at a given temperature. Applying this to the experimental configuration shown in Fig. 2 ($R = 200$ nm and $L = 1$ nm), the results yield the relaxation time to be 1.6×10^7 s at 780 K, and 43 s at 940 K (the typical value of $\tau_0 = 10^{-10}$ s was assumed, and for the temperature dependence of the magnetization the Co bulk value was used). This means that the thermally activated transition from the SD to the V state cannot be observed during measurement time (typically of 1–100 s) at 780 K or below, but the transition can be observed at 940 K, consistent with our experimental findings.

In conclusion, we investigated the magnetic stability of the vortex/single-domain states in Co nanodots. Epitaxial Co nanodots were imaged using SPLEEM. As-grown Co dots (20–800 nm wide, 1–4 nm thick) are found to be in the SD states. With annealing, we observed a magnetic phase transition from the SD to the vortex states. Based on analytical modeling and micromagnetic simulations, we proposed a new magnetic phase diagram with a broad region of bistability between both states near the phase boundary, consistent with our experimental findings. The temperature dependent energy barrier calculations further support our interpretations. The proposed concept of bistability and energy barriers between strongly nonuniform and quasiuniform magnetic states is expected to have important implications for thermally activated processes in other types of magnetic nanostructures.

This work was supported by the U.S. DOE BES-MS under Contracts No. W-31-109-ENG-38 at ANL and No. DE-AC03-76SF00098 at LBNL. H. F. D. and S. D. B. acknowledge support from the ANL-University of Chicago Consortium for Nanoscience Research (CNR).

[1] A. Aharoni, *Introduction to the Theory of Ferromagnetism* (Oxford University Press, New York, 1996).
[2] A. Hubert and R. Schäfer, *Magnetic Domains* (Springer-Verlag, Berlin, 1998).
[3] T. Shinjo, T. Okuno, R. Hassdorf, K. Shigeto, and T. Ono, Science **289**, 930 (2000).
[4] K. Y. Guslienko, Appl. Phys. Lett. **75**, 394 (1999).
[5] K. Y. Guslienko and K. L. Metlov, Phys. Rev. B **63**, 100403 (2001).
[6] H. Hoffmann and F. Steinbauer, J. Appl. Phys. **92**, 5463 (2002).
[7] L. D. Buda, I. L. Prejbeanu, U. Ebels, and K. Ounadjela, Comput. Mater. Sci. **24**, 181 (2002).
[8] R. P. Cowburn, D. K. Koltsov, A. O. Adeyeye, M. E. Welland, and D. M. Tricker, Phys. Rev. Lett. **83**, 1042 (1999).
[9] R. P. Cowburn, J. Phys. D **33**, R1 (2000).
[10] I. L. Prejbeanu *et al.*, J. Appl. Phys. **91**, 7343 (2002).
[11] A. Yamasaki, W. Wulfhekel, R. Hertel, S. Suga, and J. Kirschner, Phys. Rev. Lett. **91**, 127201 (2003).
[12] C. A. Ross *et al.*, Phys. Rev. B **65**, 144417 (2002).
[13] C. Yu, J. Pearson, and D. Li, J. Appl. Phys. **91**, 6955 (2002).
[14] T. H. Duden and E. Bauer, Surf. Rev. Lett. **5**, 1213 (1998).
[15] C. Yu, D. Li, J. Pearson, and S. D. Bader, Appl. Phys. Lett. **78**, 1228 (2001).
[16] M. J. Donahue and D. G. Porter, *OOMMF User's Guide Version 1.0* (National Institute of Standards and Technology, Gaithersburg, MD, 1999).
[17] M. Grimsditch, E. E. Fullerton, and R. L. Stamps, Phys. Rev. B **56**, 2617 (1997).
[18] W. F. Brown, Phys. Rev. **130**, 1677 (1963).
[19] Y. L. Raikher and M. I. Shliomis, Sov. Phys. JETP **40**, 526 (1974).
[20] W. T. Coffey, D. S. F. Crothers, J. L. Dormann, L. J. Geoghegan, and E. C. Kennedy, Phys. Rev. B **58**, 3249 (1998).
[21] K. Y. Guslienko, V. Novosad, Y. Otani, H. Shima, and K. Fukamichi, Appl. Phys. Lett. **78**, 3848 (2001).